

Copper(II) and Cobalt(II) Carboxylates Containing the 1,3,4-Oxadiazole Fragment: Structures and Properties

L. D. Popov^{a, *}, S. A. Borodkin^a, M. A. Kiskin^b, A. A. Pavlov^{c, **}, N. N. Efimov^b,
E. A. Ugolkova^b, V. V. Minin^{b, ***}, and I. N. Shcherbakov^a

^a Southern Federal University, Rostov-on-Don, Russia

^b Kurnakov Institute of General and Inorganic Chemistry, Russian Academy of Sciences, Moscow, Russia

^c Nesmeyanov Institute of Organoelement Compounds, Russian Academy of Sciences, Moscow, Russia

*e-mail: ldpopov@mail.ru

**e-mail: pavlov@ineos.ac.ru

***e-mail: minin@igic.ras.ru

Received February 10, 2021; revised May 24, 2021; accepted May 27, 2021

Abstract—Complexes [Cu₂L₄(MeOH)₂] (**I**) and [CoL₂] (**II**) are synthesized by the reactions of copper(II) and cobalt(II) acetates with 3-[5-*p*-tolyl]-1,3,4-oxadiazol-2-yl]acrylic acid (HL). The crystal structure of complex **I** is determined by X-ray diffraction (XRD) (CIF file CCDC no. 2052347). The crystals are monoclinic, space group *C2/c*, *a* = 26.056(4), *b* = 19.677(3), *c* = 13.998(2) Å, β = 91.571(3)°, *V* = 7175(2) Å³, ρ_{calc} = 1.026 g/cm³, *Z* = 4. In a molecule of complex **I**, the pair of centrosymmetric copper atoms is bound by four bridging carboxyl groups. The intramolecular Cu...Cu distance is 2.654(2) Å. The coordination polyhedron CuO₅ is a distorted square pyramid. The magnetic interactions between the copper(II) ions in complex **I** are shown to be antiferromagnetic (*2J* = −185 cm^{−1}). In the case of complex **II**, the application of an external magnetic field decreases the magnetic relaxation rate. The Raman mechanism and direct mechanism are the most probable route for magnetization relaxation. Unlike the copper(II) complex, complex **II** is probably mononuclear in both the solution and solid phase.

Keywords: carboxylates, magnetochemistry, NMR spectroscopy, XRD

DOI: 10.1134/S1070328422020051

INTRODUCTION

Complex formation of transition metals with polydentate organic ligands is one of the most important problems of the modern coordination chemistry. A combination of the properties of organic and inorganic substances in coordination compounds allows one to synthesize new hybrid materials and reveal the participation of metal complexes in chemical biological processes.

Metal carboxylates play an important role in coordination chemistry due to using them in diverse areas of science and technology [1, 2]. Their structures depend on both the nature of the metal and carboxylic acid and synthetic conditions [3, 4]. Metals of unsaturated carboxylates occupy a special place [5, 6]. They are used as materials for the production of photoactive agents [7–9], catalysts [10, 11], molecular magnetics [12, 13], and biomimetic models of various enzymes. Some monomeric and polymeric carboxylates are good precursors for the synthesis of nanocomposite and hybrid materials [14–18].

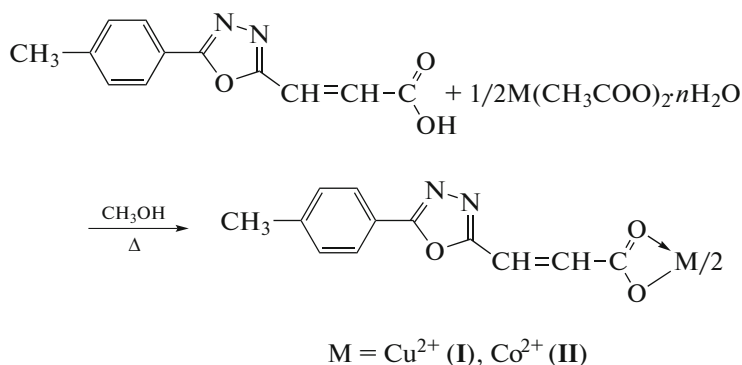
3-(5(*p*-Tolyl)-1,3,4-oxadiazol-2-yl)acrylic acid (HL) was chosen as the ligand in this work. It is well known

that the compounds containing the 1,3,4-oxadiazole fragment have pronounced biological activity [19, 20] and interesting photochemical properties [21–24]. We have previously synthesized and studied the zinc(II) [25, 26] and silver(I) [27] complexes with 1,3,4-oxadiazolylacrylic acids. Since the copper(II) complexes are good models of metalloproteins [28] and the cobalt(II) complexes can manifest anomalous magnetic properties related to the retarded relaxation of magnetic susceptibility [29, 30] and spin crossover phenomenon [31–33], the copper(II) and cobalt(II) complexes with HL, [Cu₂L₄(MeOH)₂] (**I**) and [CoL₂] (**II**), were studied in this work.

EXPERIMENTAL

Copper(II) and cobalt(II) acetates, methanol, and DMSO (reagent grade, Acros) were used.

The complexes were synthesized via the following Scheme 1:



Scheme 1.

Synthesis of complex I. A solution of copper(II) acetate monohydrate (0.086 g, 2.15 mmol) in methanol (5 mL) was added to a boiling suspension of acid HL [34] (200 g, 4.30 mmol) in methanol (10 mL). A blue precipitate formed immediately. The obtained suspension was refluxed for 5 h, filtered, washed with boiling methanol, and dried in vacuo. The yield of compound **I** was 0.098 g (51%). According to the elemental analysis data, compound **I** corresponds to the composition $\text{CuL}_2 \cdot \text{CH}_3\text{OH}$.

For $\text{C}_{25}\text{H}_{22}\text{N}_4\text{O}_7\text{Cu}$

Anal. calcd., %: C, 54.20 H, 4.00 N, 10.11 Cu, 11.47

Found, %: C, 55.60 H, 3.80 N, 10.40 Cu, 12.50

IR (ν , cm^{-1}): 3077 w, 1617 vs, 1557 m, 1532 m, 1497 s, 1407 vs, 1234 w, 1187 w, 1094 w, 978 w, 876 w, 828 w, 763 m, 613 w, 506 w, 437 w.

A single crystal of compound **I**· CH_3OH was obtained by the slow evaporation of a solution of the copper(II) complex in methanol.

Synthesis of complex II. Cobalt(II) acetate tetrahydrate (0.107 g, 2.15 mmol) in methanol (5 mL) and KOH (0.048 g, 4.30 mmol) in methanol (5 mL) were added to a boiling suspension of acid HL (0.200 g, 4.30 mmol) in methanol (10 mL). A pink precipitate formed immediately. The obtained suspension was refluxed for 5 h, filtered, washed with boiling methanol, and dried in vacuo. The yield of compound **II** was 0.120 g (71%). According to the elemental analysis data, compound **II** corresponds to CoL_2 .

For $\text{C}_{24}\text{H}_{18}\text{N}_4\text{O}_6\text{Co}$

Anal. calcd., %: C, 55.74 H, 3.48 N, 10.83 Co, 11.39

Found, %: C, 55.40 H, 3.80 N, 11.30 Co, 11.70

IR (ν , cm^{-1}): 3076 w, 1614 vs, 1585 m, 1567 m, 1497 vs, 1397 vs, 1309 w, 1262 s, 1176 w, 1092 w, 1025 w, 974 w, 837 w, 761 m, 701 w, 614 w, 503 w, 439 w.

^1H NMR (300 MHz; 293 K; DMSO; δ , ppm): 4.05 (s, 3H, CH_3), 7.51 (s, 2H, CH_{Ar}), 8.68 (s, 2H, CH_{Ar}), 12.11 (br.s, CH), 35–45 (br.s, $\text{CH}-\text{COO}$).

XRD of a single crystal of compound **I**· CH_3OH was carried out on a Bruker Apex II diffractometer equipped with a CCD detector ($\text{MoK}\alpha$, $\lambda = 0.71073 \text{ \AA}$, graphite monochromator) [35]. A semiempirical absorption correction ($T_{\text{min}}/T_{\text{max}} = 0.6055/0.7461$) was applied using the SADABS program [36]. The structure was solved by full-matrix least squares in the anisotropic approximation for all non-hydrogen atoms. The positions of the hydrogen atoms at the oxygen and carbon atoms of the organic ligands were generated geometrically and refined by the riding model. The calculations were performed using the SHELX software [37] with OLEX2 [38]. Since the solvate molecules were disordered, the XRD data were corrected by the “squeeze” method of the PLATON program [39]. A relatively low quality of the crystals (several crystals were studied) resulted in high R factors. The crystallographic parameters and structure refinement details for complex **I** at $T = 100(2) \text{ K}$ are as follows: $\text{C}_{50}\text{H}_{44}\text{Cu}_2\text{N}_8\text{O}_{14}$, $M = 1108.00 \text{ g/mol}$, space group $C2/c$, green needle-like crystal, $0.30 \times 0.05 \times 0.05 \text{ mm}$, $a = 26.056(4)$, $b = 19.677(3)$, $c = 13.998(2) \text{ \AA}$, $\beta = 91.571(3)^\circ$, $V = 7175(2) \text{ \AA}^3$, $Z = 4$, $\rho_{\text{calc}} = 1.026 \text{ g cm}^{-3}$, $\mu = 0.645 \text{ mm}^{-1}$, $1.30^\circ \leq \theta \leq 26.37^\circ$, sphere segment $-32 \leq h \leq 32$, $-24 \leq k \leq 24$, $-17 \leq l \leq 17$, 27213 measured reflections, 7341 independent reflections, 4687 reflections with $I > 2.0\sigma(I)$, $R_{\text{int}} = 0.0893$, $\text{GOOF} = 1.231$, $R_1 (I > 2\sigma(I)) = 0.1433$, $wR_2 (I > 2\sigma(I)) = 0.4306$, R_1 (all data) = 0.1855, wR_2 (all data) = 0.4609, $\Delta\rho_{\text{min}}/\Delta\rho_{\text{max}}$, $e \text{ \AA}^{-3} = -1.866/3.962$.

The structural parameters were deposited with the Cambridge Crystallographic Data Centre (CIF file CCDC no. 2052347; deposit@ccdc.cam.ac.uk or http://www.ccdc.cam.ac.uk/data_request/cif).

NMR spectra were recorded on a Bruker Avance 300 spectrometer (working frequency for ^1H 300.13 MHz). Chemical shifts (δ , ppm) were deter-

mined relative to the residual signal of DMSO used as the solvent (^1H , 2.50 ppm).

EPR spectra were detected on a BRUKER Elexsys E680X EPR spectrometer in the X range (frequency ~ 9.8 GHz) at room temperature (297 K).

The magnetic behavior of the complexes was studied by the static and dynamic magnetic susceptibility methods using the PPMS-9 Quantum Design automated complex for physical measurements with the option for measuring magnetic properties. This instrument makes it possible to perform measurements in a temperature range of 2–300 K in constant magnetic fields with the intensity up to 9 T. Variable magnetic fields with an amplitude of 5, 3, and 1 Oe for the frequency ranges 10–100, 100–1000, and 10–10000 Hz, respectively, were used for studies of the dynamic magnetic susceptibility. These measurement conditions make it possible to avoid heating at low temperatures (which can take place at high amplitude and modulation frequency) and to obtain the best signal-to-noise ratio. The magnetic behavior was studied on polycrystalline samples wetted with Nujol (to avoid the orientation of crystallites in the magnetic field) and sealed in polyethylene packets [40]. The paramagnetic component of the magnetic susceptibility (χ) was determined with allowance for the diamagnetic contribution of the sample itself estimated from Pascal's constants and magnetic contributions of the sample holder and Nujol.

RESULTS AND DISCUSSION

The reactions of cobalt(II) and copper(II) acetates with HL afford complexes with the composition ML_2 . In the IR spectra of the complexes (compared to the IR spectrum of the ligand), the absorption band of the OH group stretching vibrations (which is observed at 2500–2600 cm^{-1} in the spectrum of HL) disappears and the frequency of the C=O group stretching vibrations decreases considerably (by ~ 100 cm^{-1}), indicating the coordination of the carbonyl group to the metal ion. The structure of complex **I** is a classical binuclear tetracarboxylate-bonded copper(II) dimer in which the inversion center is arranged between the copper atoms (Cu...Cu 2.654(2) Å) (Fig. 1). The oxygen atoms of the carboxylate groups (Cu–O 1.948(7)–1.968(7) Å; OCuO 88.8(3) $^\circ$ –90.1(3) $^\circ$, 167.8(3) $^\circ$, and 168.3(3) $^\circ$) lie in the base of the CuO_5 square pyramid ($\tau = 0.008$ [41], the Cu(1) atom shifts from the O_4 plane by 0.20 Å). The oxygen atom of the methanol molecule is localized at the vertex of the pyramid (Cu–O 2.134(7) Å). The Cu...Cu and Cu–O distances are analogous to those observed in similar binuclear complexes [42, 43]. In both L, the carboxyl group and oxodiazole fragment lie in one plane (the average deviation of the atoms from the plane is less than 0.088 Å). The angle between the aforementioned plane and benzene ring is 11.7 $^\circ$ and 23.4 $^\circ$, respectively.

The π – π -stacking interactions are observed in the crystal between the oxodiazole cycle (O(3)C(4)N(1)N(2)C(5)) and phenyl fragment of the adjacent molecule of the complex (C(6)–C(11), 1 – x , 1 – y , 1 – z): the distance between the centroids is 3.730(6) Å, the angle between the planes is 6.5(5) $^\circ$, and the shortest distance between the atoms of the rings is 3.572(4) Å. The interactions lead to the formation of a supramolecular three-dimensional porous structure, the cavities of which are filled with the disordered solvate molecules (Fig. 2).

The static magnetic susceptibility of the complexes was measured in a temperature range of 2–300 K in the external magnetic field with an intensity of 5000 Oe (Fig. 3). The behaviors observed for complexes **II** and **I** are basically different.

The value of χT for compound **II** based on one metal atom is 1.40 $\text{cm}^3 \text{K mol}^{-1}$ at 300 K, which is appreciably lower than the value characteristic of the noninteracting Co^{2+} ion in the high-spin state ($3d^7$, $^4F_{9/2}$, $\chi T = 1.875 \text{ cm}^3 \text{K mol}^{-1}$) [44]. On cooling compound **II**, the values of χT decrease smoothly to 1.19 $\text{cm}^3 \text{K mol}^{-1}$ at 100 K and then decrease more sharply down to 0.62 $\text{cm}^3 \text{K mol}^{-1}$ at 2 K. It should be mentioned that the Co(II) complexes are more characterized by an overestimation of the experimental values over theoretical ones due to a noticeable spin-orbital interaction. The magnetic behavior of complex **II** can indicate appreciable interactions of the antiferromagnetic type, strong magnetic anisotropy, or a significant fraction of the cobalt ions in the low-spin state.

For complex **I** at 300 K, χT is 0.57 $\text{cm}^3 \text{K mol}^{-1}$ based on two metal atoms. This value is noticeably lower than that characteristic of two noninteracting Cu^{2+} ions ($3d^9$, $^2D_{5/2}$, $\chi T = 0.76 \text{ cm}^3 \text{K mol}^{-1}$). With decreasing temperature, χT decreases uniformly to 0.08 $\text{cm}^3 \text{K mol}^{-1}$ at 100 K, and then a smoother decrease is observed down to 0.02 $\text{cm}^3 \text{K mol}^{-1}$ at 2 K. This dependence is typical of the exchange-bound binuclear copper complexes. In order to determine the exchange interaction parameter, the experimental dependence $\chi T(T)$ was approximated by the Bleaney–Bowers equation

$$\chi = \left(Ng^2 \mu_B^2 / 3kT \right) \left[1 + (1/3) \exp \{ -2J/kT \} \right]^{-1},$$

where N is Avogadro's number, g is the copper ion factor, μ_B is Bohr's magneton, k is the Boltzmann constant, and J is the exchange parameter. According to the EPR spectroscopic data, the values of $g_{\text{iso}} = (g_x + g_y + g_z)/3$ can be used as the g factor when modeling the temperature dependence of the static magnetic susceptibility in order to minimize fitting parameters and obtain more real values of other approximation parameters. In the case of complex **I**, $g_{\text{iso}} = 2.134$. The exchange integral was found to be $2J = -185 \text{ cm}^{-1}$ ($R^2 = 0.9898$) as a sequence of the best approximation

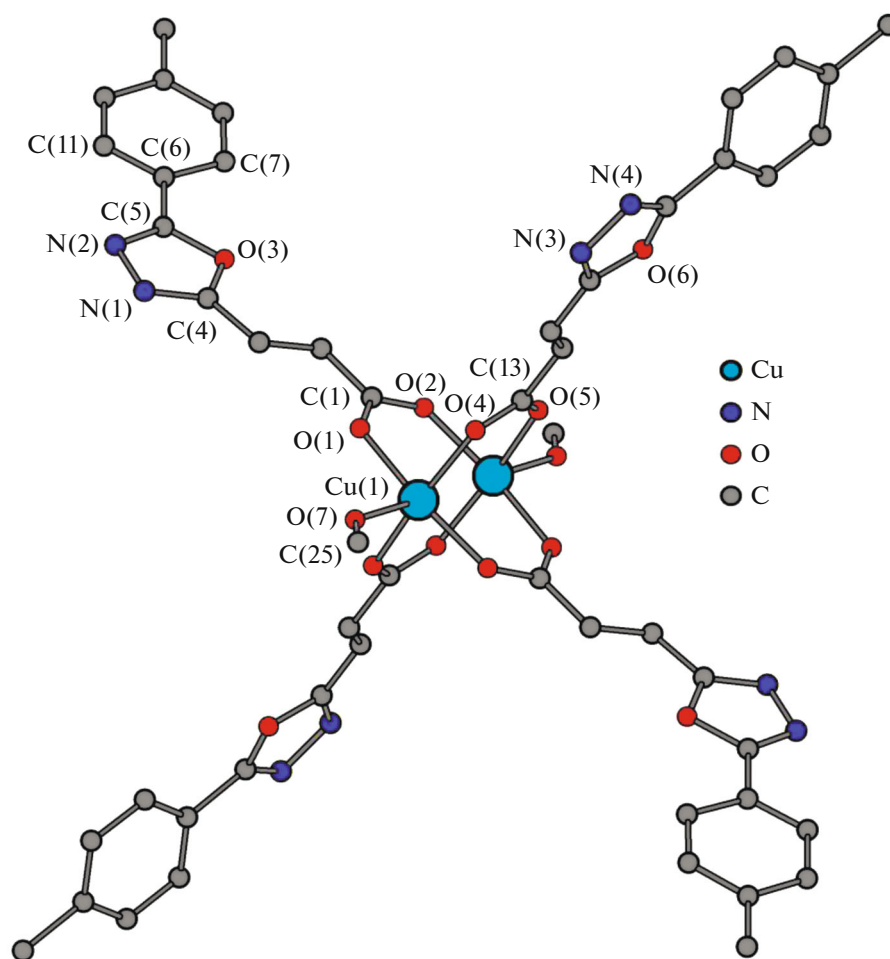


Fig. 1. Molecular structure of complex I.

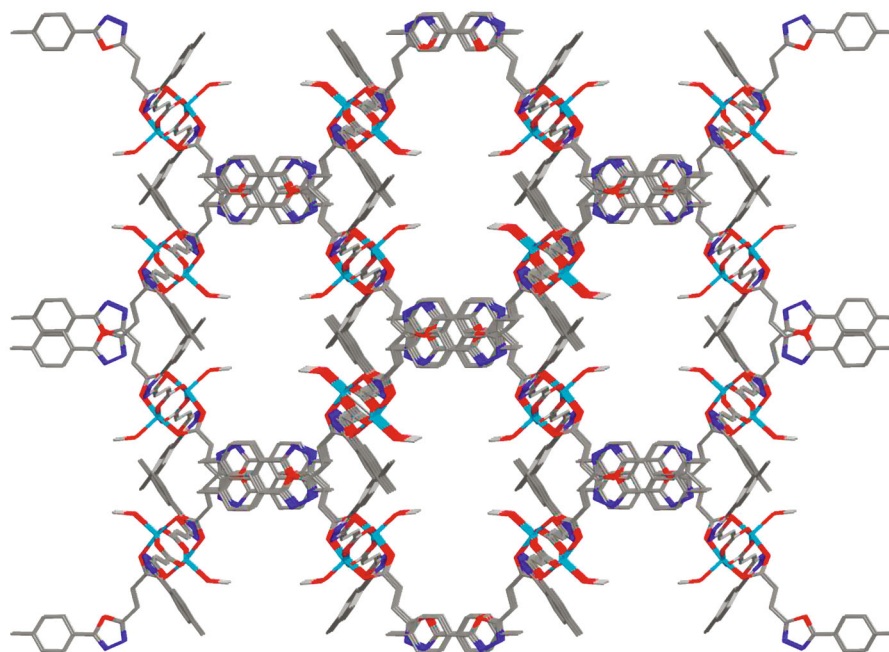


Fig. 2. Fragment of the packing of molecules of complex I in the crystal.

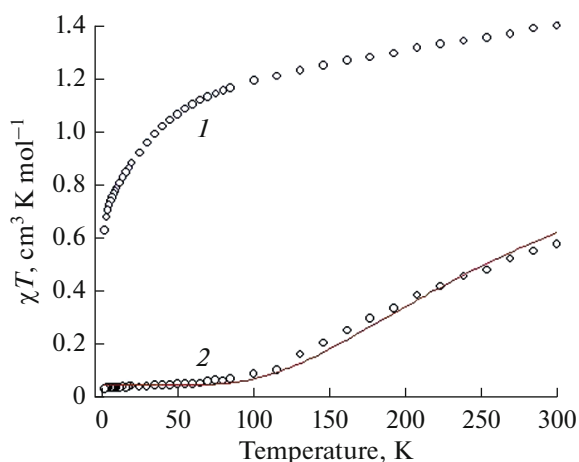


Fig. 3. Temperature dependences of χT for compounds (1) **II** (based on one metal atom) and (2) **I** (based on two metal atoms) in a magnetic field of 5000 Oe. Line is the theoretical curve with the parameters indicated in the text.

of the theoretical curve to the experimental data and taking into account the possible presence of a monomeric impurity. The content of the monomer impurity in the studied sample did not exceed 5%. The static magnetic susceptibility data unambiguously confirm the binuclear structure of complex **I** [45–47].

It is known that complexes containing anisotropic ions can manifest the properties of single-molecule magnets (SMM), which implies the slow relaxation of magnetization. The complexes containing the high-spin Co^{2+} ion are most promising among complexes with $3d$ -metal ions [48–52].

The dynamic magnetic susceptibility was measured to determine the relaxation times of magnetization of the cobalt ions in complex **II**. The measurements in the zero magnetic field showed the absence of a signal different from zero on the frequency dependence of

the imaginary component of the dynamic magnetic susceptibility χ'' even at 2 K (Fig. 4), indicating a short relaxation time of magnetization of the complex. The application of an external magnetic field can substantially increase the relaxation time of magnetization because of a decrease in the influence of the quantum tunneling (QT) effect. An increase in the relaxation time can provide a possibility to observe a slow magnetization relaxation in a frequency range of 10–10000 Hz accessible to the equipment used.

In the case of complex **II**, the application of an external magnetic field decreases the magnetic relaxation rate, which makes it possible to observe the values different from zero with a maximum on the dependences of χ'' on the frequency of the oscillating magnetic field. In order to determine the temperature dependence of the relaxation time, the isotherms of the frequency dependences of the dynamic magnetic susceptibility were measured at the optimum magnetic field intensity when the relaxation time of magnetization is longest. The longest relaxation time corresponds to the lowest frequency of the oscillating magnetic field to which the maximum of the frequency dependence of the imaginary component of the dynamic magnetic susceptibility corresponds. The intensity of the constant magnetic field for complex **II** turned out to be 2500 Oe due to measuring the dynamics of the magnetic behavior of the complex in magnetic fields of different intensities (Fig. 5). The relaxation times at fixed temperatures were determined using the approximation of the experimental data by the generalized Debye model (lines χ'' in Fig. 5).

The experimental values of the relaxation time vs. inverse temperature plotted in the semilogarithmic coordinates do not lie on one straight line (Fig. 6), indicating that there are routes of magnetization different from the Orbach mechanism ($\tau = \tau_0 \exp\{\Delta E/k_B T\}$, Arrhenius equation). The high-temperature (2.75–3.5 K) part of the $\tau(1/T)$ dependence was approximated by the Arrhe-

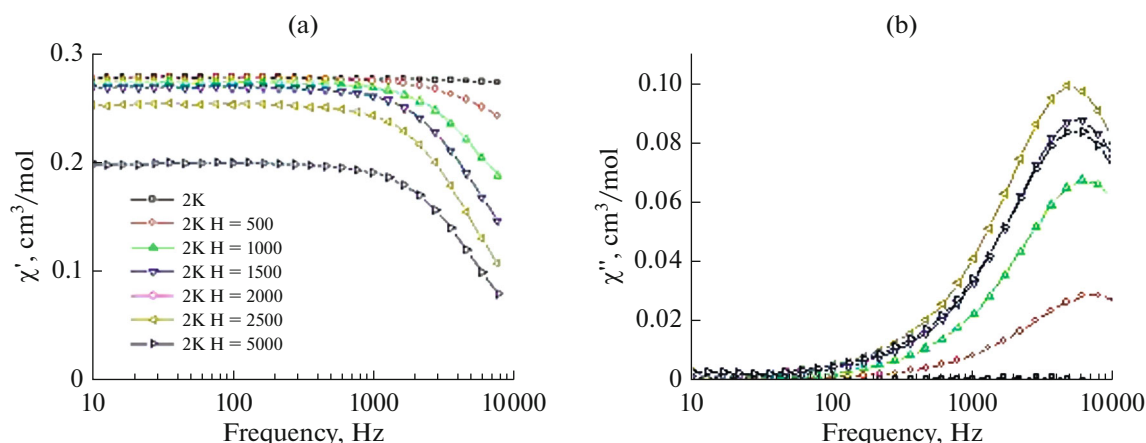


Fig. 4. Frequency dependences of the (a) real (χ') and (b) imaginary (χ'') components of the dynamic magnetic susceptibility of sample **II** at different magnetic field intensities; $T = 2$ K.

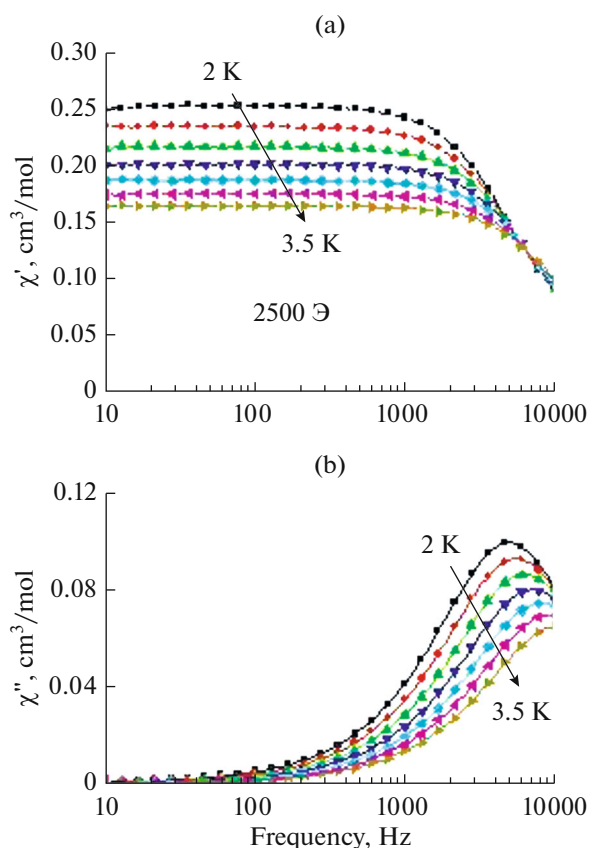


Fig. 5. Frequency dependences of the (a) real (χ') and (b) imaginary (χ'') components of the dynamic magnetic susceptibility of sample **II** in the temperature range 2–3.5 K (increment 0.25 K) at a magnetic field intensity of 2500 Oe.

nius equation in order to compare the results of our study with other works devoted to studying the dynamics of the magnetic behavior of the cobalt complexes. The best approximation of the theoretical curve to the experimental data was obtained at the following parameters: $\tau_0 = 4.1 \times 10^{-6}$ s and $\Delta E/k_B = 5$ K.

In order to establish the most probable relaxation routes of magnetization for complex **II**, the temperature dependence of the relaxation time was approximated in the whole temperature range using possible relaxation mechanisms. When analyzing the experimental data, the Raman relaxation mechanism ($\tau_{\text{Raman}}^{-1} = C_{\text{Raman}} T^{n_{\text{Raman}}}$, where C_{Raman} and n_{Raman} are the parameters of the Raman relaxation parameters), QT mechanism ($\tau_{\text{KT}}^{-1} = B_{\text{QT}}$, where B_{QT} is the relaxation rate via the QT mechanism), and direct relaxation mechanism ($\tau_{\text{direct}}^{-1} = A_{\text{direct}} H^A T$, A_{direct} is the parameter of the direct relaxation mechanism), and their linear combinations were used along with the Orbach relaxation mechanism. The experimental data

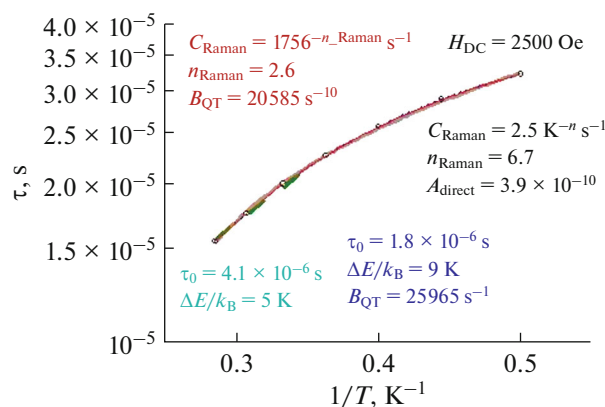


Fig. 6. Dependences of the relaxation time on the inverse temperature $\tau(1/T)$ for complex **II** at an optimum magnetic field intensity of 2500 Oe. Red solid line is the approximation by the sum of the Raman and QT relaxation mechanisms; blue dashed line is the approximation by the sum of the Orbach and QT mechanisms; green dashed line is the approximation of the high-temperature range (2.75–3.5 K) by the Arrhenius equation; and green solid line is the approximation by the sum of the direct and Raman relaxation mechanisms.

are described most satisfactorily by the dependences determined by the sum of the Raman and QT relaxation mechanisms with the parameters $C_{\text{Raman}} = 1756 \text{ K}^{-n_{\text{Raman}}} \text{ s}^{-1}$, $n_{\text{Raman}} = 2.6$, and $B_{\text{QT}} = 20585 \text{ s}^{-1}$; the sum of the Orbach and QT relaxation mechanisms with the parameters $\tau_0 = 1.8 \times 10^{-6}$ s, $\Delta E/k_B = 9$ K, and $B_{\text{QT}} = 25965 \text{ s}^{-1}$; and the sum of the direct mechanism and the Raman relaxation mechanism with the parameters $C_{\text{Raman}} = 2.5 \text{ K}^{-n_{\text{Raman}}} \text{ s}^{-1}$, $n_{\text{Raman}} = 6.7$, and $A_{\text{direct}} = 3.9 \times 10^{-6} \text{ K}^{-1} \text{ Oe}^{-4} \text{ s}^{-1}$ (Fig. 6). The use of other relaxation mechanisms and their combinations results in an excessive parametrization or unsatisfactory correspondence between the theoretical curve and experimental data.

Sometimes the QT effect is not suppressed even by a sufficiently strong magnetic field. However, as mentioned above, the external magnetic field application noticeably affects the relaxation rate of the complex decreasing the rate. Therefore, it can be asserted that the QT mechanism is not involved in the relaxation of the magnetization of the cobalt ion of complex **II** in a field of 2500 Oe.

For complex **II**, the preexponential factor is $\tau_0 \approx 10^{-6}$ s if taking into account the Orbach relaxation mechanism. The relaxation times characteristic of the overbarrier one-phonon magnetization reversal corresponding to the Orbach mechanism should take values of $\sim 10^{-10} - 10^{-12}$ s [53]. The use of the sum of the direct mechanism and Raman relaxation mechanism gives the most convincing description of the experimental

dependence $\tau(1/T)$ from the viewpoint of the parameters of the theoretical model.

Therefore, the Raman mechanism and direct mechanism are the most probable route for the magnetization relaxation of complex **II**.

EPR spectroscopy makes it possible to establish unpaired electrons in coordination compounds and determine the structure of the coordination sphere of the ion containing unpaired electrons. The complexes containing Cu^{2+} ions are excellent objects for studying using EPR spectroscopy. In particular, the mono/binuclear structure of complexes of this ion can unambiguously be distinguished using EPR [54].

The EPR spectrum of complex **I** (Fig. 7) is a superposition of the signal of the copper dimer (spin $S = 1$) with the fine structure and the spectrum of the mononuclear copper(II) complex ($S = 1/2$; signal in the magnetic field range ~ 350 mT). The signal of the mononuclear copper(II) complex ($S = 1/2$) is well consistent with the studies by the static magnetic susceptibility method. The axial spin-Hamiltonian with the fine structure was used for the theoretical description of the spectrum of the copper dimer

$$H = \beta(g_x S_x H_x + g_y S_y H_y + g_z H_z S_z) + D(S_z^2 - S(S+1)/3),$$

where $S = 1$; S_x , S_y , and S_z are the projections of the full spin on the x , y , and z axes, respectively; D is the component of the fine interaction tensor; g_x , g_y , and g_z are the components of the g tensor; and H is the applied magnetic field.

The EPR spectrum described by the spin-Hamiltonian was simulated using the eigenfield method [55]. The best coincidence between the experimental data and theoretical curve was obtained for the parameters presented in the caption to Fig. 7.

At room temperature, the EPR spectrum of complex **II** represents a broad unresolved line. An EPR signal can be observed at room temperature only if the Co^{2+} ion in the compound is low-spin. This is confirmed by the static magnetic susceptibility data on the coexistence of the high-spin and low-spin cobalt compounds in the studied substance.

Cobalt complex **II** was tested to the spin crossover effect by NMR. The ^1H NMR spectrum of complex **II** (Fig. 8) exhibits a strong signal broadening, ^1H chemical shift values of several tens ppm uncharacteristic of diamagnetic spectra, and a change in these values with temperature (as a consequence of the Curie law), which significantly indicates the paramagnetic nature of the studied sample. As a rule, the nuclear relaxation rate (and, hence, broadening) is related to the remoteness of the core from the paramagnetic center [56]. This regularity is also observed in the spectrum of compound **II**: the signal of the methyl group is least broadened (the full width at $1/2h_{\text{max}}$ is 8.0 Hz), the signals of the phenyl fragment protons are more broad-

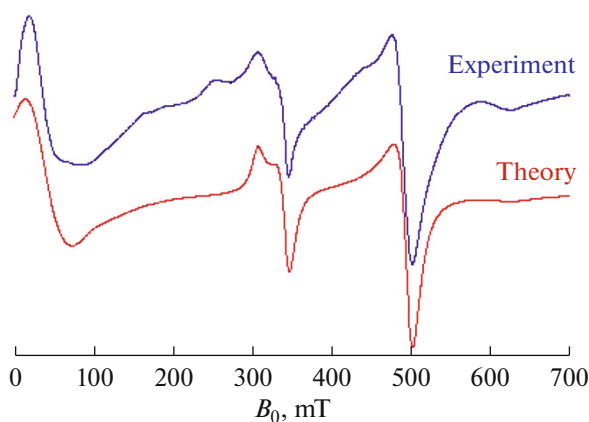


Fig. 7. Spectrum of compound **I** (powder) at 293 K. Parameters of the theoretical model: $S = 1$, $C = 85.7\%$, $|D| = 0.3512 \text{ cm}^{-1}$, $g_z = 2.320$, $g_x = 2.042$, $g_y = 2.040$; $S = 1/2$, $C = 14.3\%$, $g_z = 2.300$, $g_x = 2.055$, $g_y = 2.055$.

ened (18.5 and 27.1 Hz), and the signals of the CH protons are broadened to the highest extent (~ 550 and 4000 Hz), which makes them poorly discernible in the spectrum. Thus, the number, integral intensities, and relaxation characteristics of the signals in the ^1H NMR spectrum of complex **II** correspond to the composition of the complex, indicating its stability in a DMSO solution. In addition, a decrease in the paramagnetic shifts with increasing temperature indicates that no spin transition occurs in the studied temperature range from 293–340 K [57]. Thus, no spin crossover is observed for this compound.

ACKNOWLEDGMENTS

The XRD, magnetic, and EPR studies were carried out using the equipment of the Center for Collective Use “Physical Methods of Investigation” at the Kurnakov Institute of General and Inorganic Chemistry (Russian Academy of Sciences) supported by the state assignment of the Kurnakov Institute of General and Inorganic Chemistry (Russian Academy of Sciences) in the area of basic research.

FUNDING

The NMR studies were performed under the support of the Russian Science Foundation (project no. 20-73-00194) using the equipment of the Center for Molecular Composition Studies at the Nesmeyanov Institute of Organoelement Compounds (Russian Academy of Sciences).

CONFLICT OF INTEREST

The authors declare that they have no conflicts of interest.

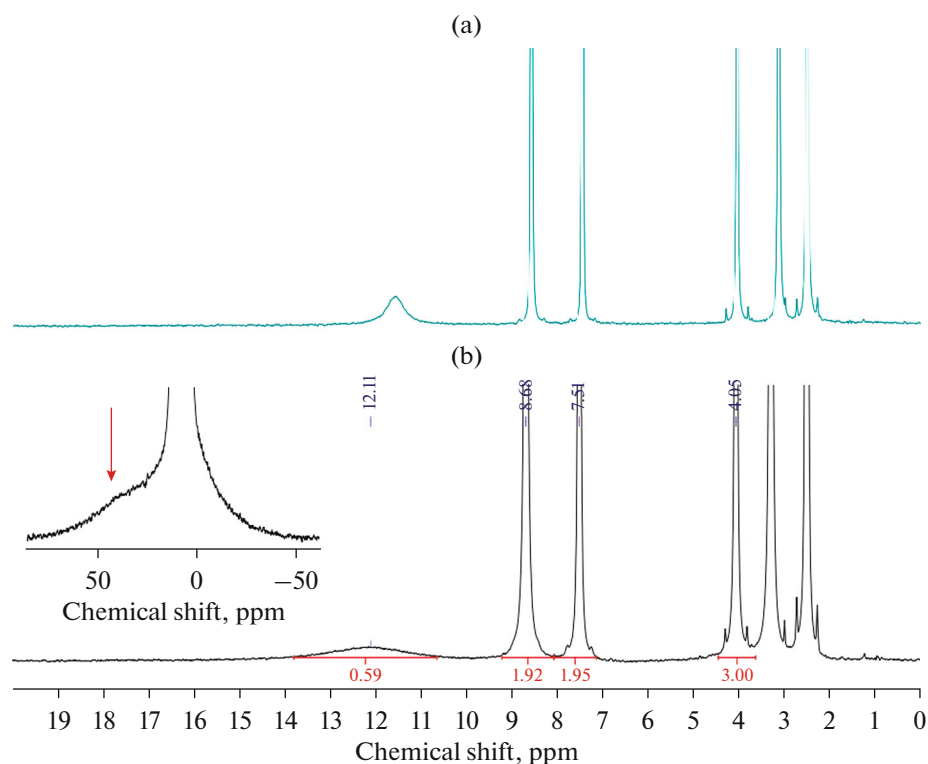


Fig. 8. ^1H NMR spectra of complex **II** recorded at (a) 293 and (b) 340 K.

REFERENCES

- Pomogailo, A.D. and Dzhardimalieva, G.I. *Monoimernye i polimernye karboksilyaty metallov* (Monomeric and Polymeric Metal Carboxylates), Moscow: Fizmatlit, 2009.
- Tokito, S., Noda, K., Tanaka, H., et al., *Synth. Met.*, 2000, vols. 111–112, p. 393.
- Mehrotra, R.C. and Bohra, R., *Metal Carboxylates*, London: Academic Press, 1983.
- Kiskin, M.A. and Eremenko, I.L., *Usp. Khim.*, 2006, vol. 75, p. 627.
- Dzhardimalieva, G.I. and Pomogailo, A.D., *Usp. Khim.*, 2008, vol. 77, p. 270.
- Schubert, U., *Chem. Mater.*, 2001, vol. 13, p. 3487.
- Petukhova, M.V., Petrochenkova, N.V., Mirochnik, A.G., et al., *Vysokomol. Soed. B.*, 2000, vol. 44, p. 1267.
- Ling, Q.D., Cai, Q.L., Kang, E.T., et al., *J. Mater. Chem.*, 2004, vol. 14, p. 2741.
- Ling, Q., Yang, M., Wu, Z., et al., *Polymer*, 2001, vol. 42, p. 4605.
- Metal Complexes and Metals in Macromolecules*, Wohrle, D. and Pomogailo, A.D., Eds., Wiley VCH, 2003, p. 667.
- Supported Catalysts and Their Applications*, Sherrington, D.C. and Kubert, A.P., Eds., Cambridge: Royal Soc. Chem., 2001, p. 250.
- Shcherbakov, I.N., Ivanova, T.M., Kiskin, M.A., et al., *Inorg. Chim. Acta*, 2014, vol. 421, p. 507.
- Ivanova, T.M., Maslakov, K.I., Linko, R.V., et al., *Russ. J. Inorg. Chem.*, 2014, vol. 59, no. 7, p. 670. <https://doi.org/10.1134/S0036023614070067>
- Liu, G., Yan, X., Lu, Z., et al., *Chem. Mater.*, 2005, vol. 17, p. 4985.
- Hu, N.X., Esteghamatian, M., Xie, S., et al., *Adv. Mater.*, 1999, vol. 11, no. 17, p. 1460.
- Gao, M.Y., Yang, Y., Yang, B., et al., *Chem. Commun.*, 1994, p. 2779.
- Volkov, A.V., Moskvina, M.A., Karachevtsev I.V., et al., *Vysokomol. soed. A.*, 1998, vol. 40, p. 45.
- Uflyand, I.E., Shcherbakov, I.N., Popov, L.D., et al., *J. Coord. Chem.*, 2020, vol. 73, no. 24, p. 3465.
- Mazumder, S.A., Yar, M.S., Mazumder, R., et al., *Synth. Commun. Rev.*, 2017, vol. 47, no. 20, p. 1805.
- Popov, L.D., Zubenko, A.A., Fetisov, L.N., et al., *Bioorg. Khim.*, 2018, vol. 44, no. 2, p. 225.
- Feng, L., Wang, X., and Chen, Z., *Spectrochim. Acta, Part A*, 2008, vol. 71, no. 2, p. 312.
- Huaijun Tang, Hao Tang, Zhiguo Zhang, Jibing Yuan, Changjie Cong, and Keli Zhang, *Synth. Met.*, 2009, vol. 159, p. 72. <https://doi.org/10.1016/j.synthmet.2008.07.025>
- Mikhailov, I.E., Popov, L.D., Vikrishchuk, N.E., et al., *Russ. J. Gen. Chem.*, 2015, vol. 85, no. 1, p. 203.
- Mikhailov, I.E., Artyushkina, Yu.M., Dushenko, G.A., et al., *Russ. J. Gen. Chem.*, 2018, vol. 88, no. 3, p. 602.
- Mikhailov, I.E., Popov, L.D., Dushenko, G.A., et al., *Russ. J. Gen. Chem.*, 2018, vol. 88, no. 4, p. 846.

26. Mikhailov, I.E., Popov, L.D., Tkachev, V.V., et al., *J. Mol. Struct.*, 2018, vol. 1157, p. 374.
27. Kokunov, Yu.V., Gorbunova, Yu.E., Popov, L.D., et al., *Russ. J. Coord. Chem.*, 2016, vol. 42, no. 6, p. 361. <https://doi.org/10.1134/S1070328416060038>
28. Uraev A.I., *Doctoral Sci. (Chem.) Dissertation*, Rostov-on-Don, 2014.
29. Tupolova, Y.P., Shcherbakov, I.N., Popov, L.D., et al., *Dalton Trans.*, 2019, vol. 48, no. 20, p. 6960.
30. Tupolova, Y.P., Shcherbakov, I.N., Korchagin, D.V., et al., *J. Phys. Chem.*, 2020, vol. 124, no. 47, p. 25957.
31. Goodwin, H.A., *Top. Curr. Chem.*, 2004, vol. 234, p. 23.
32. Murray, K.S., *Eur. J. Inorg. Chem.*, 2008, no. 20, p. 3101.
33. Pavlov, A.A., Denisov, G.L., Kiskin, M.A., et al., *Inorg. Chem.*, 2017, vol. 56, p. 14759.
34. Rozhkov, S.S., Ovchinnikov, K.L., Kraskovskaya, G.G., et al., *Russ. J. Org. Chem.*, 2015, vol. 51, no. 7, p. 982.
35. *SMART (control) and SAINT (integration) Software. Version 5.0*, Madison: Bruker AXS Inc., 1997.
36. Krause, L., Herbst-Irmer, R., Sheldrick, G.M., and Stalke, D., *J. Appl. Crystallogr.*, 2015, vol. 48, p. 3.
37. Sheldrick, G., *Acta Crystallogr., Sect. A: Found. Crystallogr.*, 2007, vol. 64, p. 112.
38. Dolomanov, O.V., Bourhis, L.J., Gildea, R.J., et al., *J. Appl. Crystallogr.*, 2009, vol. 42, p. 339.
39. Spek, A.L., *Acta Crystallogr., Sect. C: Struct. Chem.*, 2015, vol. 71, p. 9.
40. Petrosyants, S.P., Ilyukhin, A.B., Efimov, N.N., and Novotortsev, V.M., *Russ. J. Coord. Chem.*, 2018, vol. 44, no. 12, p. 733. <https://doi.org/10.1134/S1070328418120060>
41. Addison, A.W., Rao, T.N., Reedijk, J., et al., *Dalton Trans.*, 1984, no. 7, p. 1349.
42. Fomina, I.G., Dobrokhotova, Zh.V., Aleksandrov, G.G., et al., *Izv. Akad. Nauk., Ser. Khim.*, 2007, p. 1660.
43. Gogoleva, N.V., Aleksandrov, G.G., Pavlov, A.A., et al., *Russ. J. Coord. Chem.*, 2018, vol. 44, no. 2, p. 91. <https://doi.org/10.1134/S1070328418020057>
44. Rakitin, Yu.V. and Kalinnikov, V.T., *Sovremennaya magnetokhimiya (Modern Magnetochemistry)*, Leningrad: Nauka, 1984.
45. Lukov, V.V., Tsaturyan, A.A., Tupolova, Y.P., et al., *J. Mol. Struct.*, 2020, vol. 1199, p. 126952.
46. Kochneva I.K., Polyakova I.N., Avdeeva V.V., et al., *Dokl. Ross. Akad. Nauk.*, 2017, vol. 474, no. 5, p. 581.
47. Gusev, A.N., Nemeč, I., Herchel, R., et al., *Dalton Trans.*, 2019, no. 48, p. 3052.
48. Yambulatov, D.S., Nikolaevskii, S.A., Kiskin, M.A., et al., *Molecules*, 2020, vol. 25, no. 9, p. 2054.
49. Pavlov, A.A., Aleshin, D.Y., Savkina, S.A., et al., *ChemPhysChem.*, 2019, vol. 20, no. 8, p. 1001.
50. Pavlov, A.A., Nelyubina, Y.V., Kats, S.V., et al., *J. Phys. Chem. Lett.*, 2016, vol. 7, no. 20, p. 4111.
51. Pavlov, A.A., Savkina, S.A., Belov, A.S., et al., *Inorg. Chem.*, 2017, vol. 56, no. 12, p. 6943.
52. Varzatskii, O.A., Kats, S.V., Pavlov, A.A., et al., *Inorg. Chim. Acta*, 2018, vol. 471, p. 413.
53. Polyzou, C.D., Koumoussi, E.S., Lada, Z.G., et al., *Dalton Trans.*, 2017, vol. 46, p. 14812.
54. Rakitin, Yu.V., Larin, G.M., and Minin, V.V., *Interpretatsiya spektrov EPR koordinatsionnykh soedinenii (Interpretation of ESR Spectra of Coordination Compounds)*, Moscow: Nauka, 1993.
55. Belford, G., Belford, R.L., and Burkhaven, J.F., *J. Magn. Res.*, 1973, vol. 251, no. 11, p. 2749.
56. Solomon, I., *Phys. Rev.*, 1955, vol. 99, p. 559.
57. Pavlov, A.A., Denisov, G.L., Kiskin, M.A., et al., *Inorg. Chem.*, 2017, vol. 56, no. 24, p. 14759.

Translated by E. Yablonskaya